Hindawi
International Journal of Antennas and Propagation
Volume 2019, Article ID 2164716, 11 pages
https://doi.org/10.1155/2019/2164716

Research Article

Experimental Investigation of a Planar Antenna with Band Rejection Features for Ultra-Wide Band (UWB) Wireless Networks

Muhammad Irshad Khan,[1] Muhammad Irfan Khattak,[1] Gunawan Witjaksono,[2] Zaka Ullah Barki,[2] Sadiq Ullah,[3] Imran Khan,[1] and Byung Moo Lee[4]

[1]*Department of Electrical Engineering, University of Engineering & Technology, Peshawar, Pakistan*
[2]*Electrical & Electronic Engineering Department Universiti Teknologi PETRONAS 32610 Seri Iskandar, Perak Darul Ridzuan, Malaysia*
[3]*Department of Telecommunication Engineering, University of Engineering & Technology, Mardan, Charsadda Road, Mardan 23200, Pakistan*
[4]*School of Intelligent Mechatronics Engineering, Sejong University, Seoul 05006, Republic of Korea*

Correspondence should be addressed to Byung Moo Lee; blee@sejong.ac.kr

Received 7 February 2019; Accepted 5 May 2019; Published 2 June 2019

Academic Editor: Seong-Youp Suh

The Federal Communication Commission (FCC) has authorized the use of unlicensed ultra-wide band (UWB) spectrum in the frequency range from 3.1 to 10.6 GHz for a variety of short-range applications, including wireless monitors and printers, camcorders, radar imaging, and personal area networks (PANS). However, the interference between coexisting narrowband channels and UWB signals that share the same spectrum should be avoided by designing UWB antennas with band notch characteristics. This work presents a printed monopole antenna (PMA) with slots of different shapes etched in the radiating element to obtain band rejection in the three coexisting communication bands, i.e., Worldwide Interoperability for Microwave Access (WiMAX), Wireless Local Area Network (WLAN), and International Telecommunication Union (ITU). A rectangular slot is etched to reject the WiMAX band (3.01-3.68 GHz), an upturned C slot stops the WLAN band (5.18-5.73 GHz) while an inverted-U slot halts the ITU frequency band (7.7-8.5 GHz). The proposed antenna occupies a volume of 32 x 30 x 1.6 mm^3 and it radiates efficiently (>90%) with a satisfactory gain (>1.95 dBi) in the unnotched UWB frequency range. The simulations are performed in High Frequency System Simulator (HFSS), while the measurements are conducted in antenna measurement facility and found in close agreement with the former.

1. Introduction

Printed Monopole Antennas (PMAs) have been used in various applications of wireless communication such as radar, cognitive radio, and indoor positioning because of their affordability, wider bandwidth, and design flexibility [1, 2]. PMAs have various geometries but the most common shapes of PMAs used by researchers for UWB applications [3–6] are rectangular, circular, square, triangular, elliptical, and hexagonal. The Federal Communication Commission has authorized UWB range from 3.1to 10.6 GHz for commercial applications in 2002 [7]. High bandwidth and short-range communication is possible through UWB technology which covers a large portion of the radio spectrum [8]. Due to large bandwidth, high data rates of approximately 480 Mbps to 1.6 Gbps are achieved with good time domain impulse performance [9]. Due to these advantages, UWB technology has been able to attract interest of the researchers around the globe and the technology has been adopted widely for numerous applications. But there is an issue inherently associated with UWB communications, which is the interference of various narrow communication bands. The existing narrow bands are IEEE 802.16 WiMAX at 3.5 GHz (3.3–3.7 GHz), IEEE 802.11a WLAN at 5.2/5.8 GHz (5.15–5.82 GHz), and ITU at 8 GHz (8.025–8.5 GHz). So, the intent of this paper is to design a novel UWB PMA with notched characteristics

to stop these three communication bands to resolve the interference issue. The band-notched characteristics in UWB antennas are obtained by using various techniques such as slots in the feed line, ground, or radiator [10, 11]. Till now researchers have applied various techniques to obtain single [12–17], dual [18–25], and triple [26–28] band-notching of narrowband channels operating within the UWB spectrum. In [12] a $50 \times 42\,\text{mm}^2$ UWB antenna has been designed to suppress or notch the WiMAX frequency band (3.3-3.8 GHz) by using electromagnetic bandgap structures. The methods for notching the WLAN band (5.1-5.8 GHz) have been discussed in [13–17]. These methods include the use of E-shaped [13] and H-shaped [14] slots etched in the radiating element and feedline, respectively. The use of parasitic strip [15] near the radiating patch, split ring resonators (SRR) [16], and pin diodes [17] is also exploited to notch the WLAN band. The pin diodes need additional resources (lines and dc-supply) to operate it in the reverse/forward bias mode. The WLAN and WiMAX frequency bands have been notched by using the techniques mentioned in [18–24]. In [18] the authors have designed a $38.1 \times 24.6\,\text{mm}^2$ UWB antenna, with two T-shaped slots introduced in the radiating element to reject/notch the WLAN frequency band (5.15–5.825 GHz). Two complementary split ring resonators (CSRR) are also employed on both sides of the microstrip feedline to stop the WiMAX frequency band (3.3–3.7 GHz). In [19], slots are etched in the ground. Similarly, resonators [20] in the top layer are used for WLAN and WiMAX band rejection. Likewise, U-shaped [21], rectangular-shaped [22], H-shaped [23], and circular shaped [24] slots have been etched within the radiating element, to slash the aforementioned bands. In [25] different types of resonators have been printed on the ground plane to reject the ITU (7.8-8.4 GHz) and WLAN (5-5.4 GHz) frequency bands. In order to achieve triple band rejection within the UWB spectrum, various approaches [26–31] have been applied in the past; however controlling the bandwidth and gain of each notch band has been a challenging task. Each of the aforementioned approaches has its own pros and cons in terms of antenna size, design simplicity, and the type and number of notched frequency bands, which will be discussed in the next section.

In this work, a circular shaped ultra-wide band antenna with triple band rejection features has been presented. The overall volume of the antenna is $32 \times 30 \times 1.6\,\text{mm}^3$ which is printed on easily available and most feasible FR4 substrate material. Three slots of different size and geometrical shapes are introduced in the radiating patch to stop the WiMAX, WLAN bands, and the ITU band allocated to fixed wireless systems. The presented antenna is low-profile and relatively compact and controls the bandwidth and gain of the subject three notch bands. This antenna is a potential candidate for consideration in the existing and future UWB antennas.

The rest of the paper is organized as follows: related work is explained in Section 2. Section 3 explains the step-by-step design procedure and parametric study. Results are discussed in Section 4 whereas conclusion and future directions are outlined in Section 5.

2. Related Work

Comparison of the proposed antenna with relevant state of the art UWB antennas is presented in Table 1. The antennas presented in [12–17] are relatively larger in size and offers band-notching in a single frequency band. UWB antennas of comparable size have been proposed in [18–25]; however these designs give band-notching in two frequency bands. The UWB antennas covered in [26–31] use relatively complex mechanisms to attain band rejection in triple frequency bands.

In [26] an UWB antenna with triple band rejection features, occurring at WiMAX and lower and upper WLAN frequency bands has been proposed. The antenna in [26] occupies a comparable volume, with a decent gain; however due to the multilayer geometry the fabrication is relatively complex. The underlying core concept for band rejection in [26] is the use of ring resonators, printed on multilayer substrate to achieve rejection in the WiMAX band and lower and upper WLAN bands. In [27] horizontal and vertical stubs and open ended slots in the feedline are used to attain band rejection for WiMAX and lower and upper WLAN frequency bands. This band-notched UWB antenna has been designed using a high-permittivity dielectric substrate. In [28] a different $38.3 \times 34.5\,\text{mm}^2$ UWB antenna has been designed by incorporating rectangular and circular SRR in the radiating element and ground, respectively, to stop the coexisting, IEEE 802.11a WLAN (5.15–5.825 GHz), IEEE 802.11p Dedicated Short-Range Communications (DSRC 5.85–5.925 GHz), IEEE 802.11y (3.65 –3.69 GHz), and IEEE 802.16 WiMAX (3.3–3.8 GHz) bands. In [29], a $26.7 \times 41.5\,\text{mm}^2$ UWB antenna with a fractal defective ground surface (DGS) was proposed for multiple-input multiple-output (MIMO) applications. Rectangular and C-shaped slots were used to attain triple band rejection in 3.3–3.7 GHz, 3.7–4.2 GHz, and 5.15–5.85 GHz frequency bands. The average gain and radiation efficiency of the antenna in unnotched UWB spectrum vary from 1.13 dBi and 75%, respectively. In [30] a relatively larger ($64 \times 45\,\text{mm}^2$) UWB antenna has been proposed which is capable of band-notched features in the WiMAX, WLAN, and X-Band frequency bands. Mushroom and uniplanar electromagnetic bandgap (EBG) structures are used in the vicinity of the feedline to notch the three frequency bands. Similarly, various arrangements of Split Ring Resonator (SSR) and Complementary-SRR (CSRR) under the radiating patch and ground plane have been employed in [31] to obtain triple band-notch characteristics at WiMAX (3.3–3.7 GHz), WLAN IEEE802.11a/n (5.15–5.825 GHz), and ITU (8.025–8.4 GHz) frequency bands. The UWB antenna in [31] has a comparable size of $34 \times 32\,\text{mm}^2$ and radiate with a fair gain (>1.9 dBi); however the average radiation efficiency is <75%. Beams scanning is a useful feature desired for focussing the radiation from the UWB antenna in a specific direction. In [33] a 6-18 GHz phased array UWB antenna has been proposed, which gives a decent gain at a particular frequency and scan angle; however the limitation of this work is the absence of band-notching feature, which is sometimes essential for reducing cochannel interference with the adjacent channels.

Table 1: Comparison with diverse range of existing UWB antenna with band-notch characteristics.

Ref.	Size (mm^2)	Band Notch Technique	No. of Notched Bands	Notched Frequencies (GHz)	Major Focus/Drawback
[12]	50 ×42	Mushroom type EBG	01	WiMAX ((3.3–3.8)	UWB/bulky & single notched band
[13]	35 × 30	E-shaped slots	01	WLAN (5.15–5.35)	UWB/single notch
[14]	50 × 50	H-shaped slot	01	WLAN (5.15–5.8)	UWB/bulky & single notched band
[15]	50 ×50	Parasitic strip	01	WLAN (5.15–5.8)	-do-
[16]	48 × 48	Split Ring Resonator	01	WLAN (5.1-6)	-do-
[17]	39.8 × 50	PIN diodes	01	WLAN (5.2-5.8)	-do-
[18]	38.1 × 24.6	Slots & CSRR	02	WiMAX (3.3–3.7)/ WLAN (5.15–5.82)	UWB/two notched frequency bands
[19]	30 × 20	Truncated patch and slots in the ground	02	WiMAX (3.40-3.92)/ WLAN (5.15-5.72)	-do-
[20]	30 × 31	miniaturized resonator and Varactor diodes	02	WiMAX (3-4)/ WLAN (5.15-5.825)	-do-
[21]	33 ×32	meandered slot in the radiator and U-slot in the feed line	02	WiMAX (3.5)/ WLAN (5.6)	-do-
[25]	32 × 24	Inverted-U and Iron Shaped resonators	02	WLAN (5-5.4)/ ITU (7.8-8.4)	-do-
[26]	33 × 30	Ring resonators, printed on multi-layer substrate	03	WiMAX (3.3–3.7)/ Lower WLAN (5.15–5.35)/ Upper WLAN (5.72–5.82)	UWB/ design complexity
[27]	28.5 × 28	horizontal & vertical stubs and open-ended slots	03	WiMAX (3.3–3.6)/ lower WLAN (5.15–5.35)/ upper WLAN (5.725–5.825)	UWB/ ITU band is not notched
[28]	38.3×3 34.5	Rectangular & Circular SRR	03	WiMAX (3.28–3.82)/ WLAN (5.12–5.825)/ DSRC (5.85–5.925)	UWB/ design complexity & ITU band is not notched
[29]	41 × 26.75	Rectangular & C-shape slots	03	WiMAX (3.3– 3.7)/ C-band (3.7–4.2)/ WLAN (5.15–5.85)	UWB/ ITU band is not notched
[30]	64 × 45	EBG structures	03	WiMAX (3.3-3.6)/ WLAN (5-6)/ X-Band (7.1-7.9)	UWB/bulky
[32]	48.8 × 35.6	Rectangular slots	01	WLAN (5.15–5.85)	UWB/bulky
Proposed	32 × 30	Three slots in radiating patch	03	WiMAX (3.01-3.68)/ WLAN (5.18-5.73)/ ITU- band (7.7-8.5)	UWB

In light of the aforementioned facts and figures the proposed antenna uses a simple mechanism by inserting three slits of different geometrical shapes within the radiating element of the of the antenna to reject the three frequency bands (WiMAX, entire WLAN, and ITU band). It is worth mentioning that all these antennas radiate with a sufficient gain (>2 dBi) in the unnotched portion of the UWB spectrum. In addition, the proposed antenna has a comparable size and radiates efficiently (85-90 %) in the unnotched UWB frequency spectrum.

3. Design and Relevant Theory

3.1. Design. The proposed UWB antenna of Figure 1(d) has been obtained through the step-by-step evolution of the semicircular shape radiating structure of Figure 1(a), by inserting various types of slots (rectangular, Inverted-C, and Inverted-U) in it as shown in Figures 1(b) and 1(c), respectively. The half or semicircular disc has a radius of 13 mm, printed on a 1.6 mm thick FR4 substrate, having a loss tangent and relative permittivity of 0.02 and of 4.4,

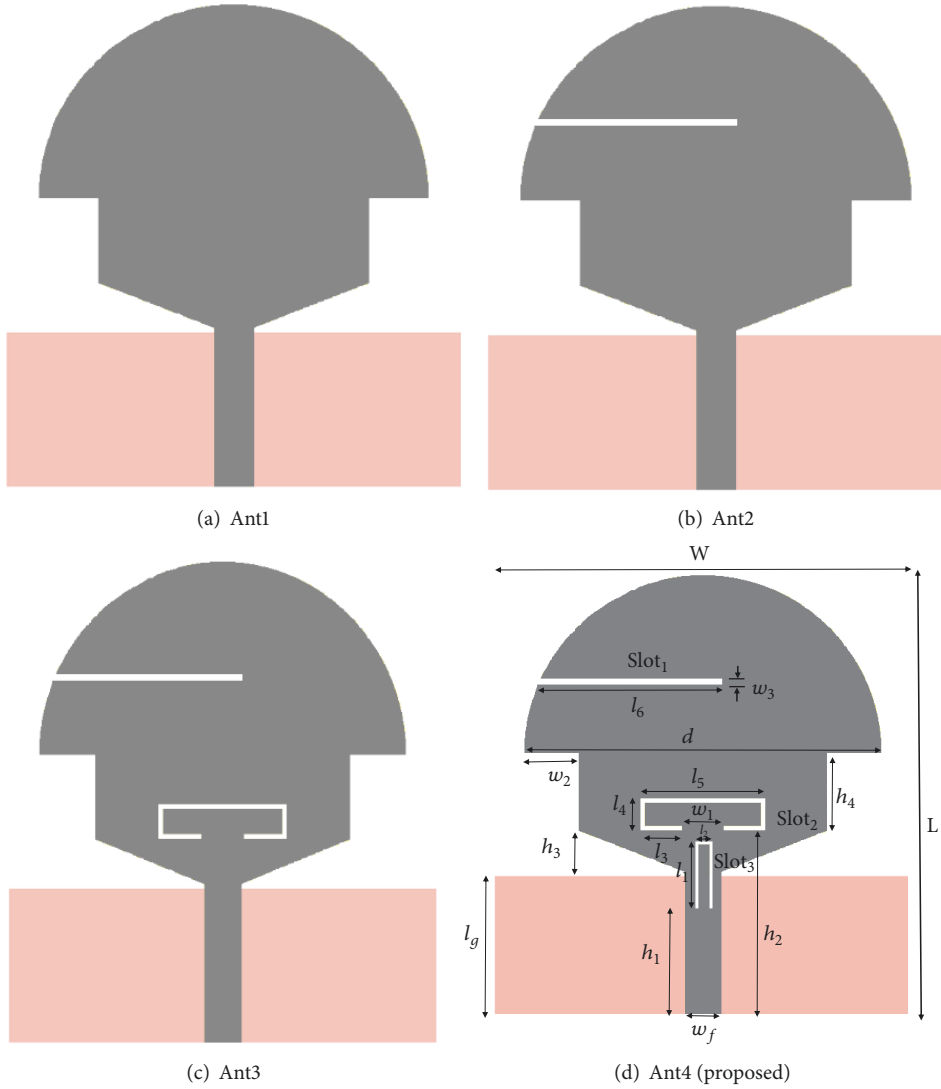

FIGURE 1: Structural evolution of the proposed UWB antenna (a) *Ant1:* UWB (3-10 GHz) (b) *Ant2:* UWB with Single Band (WiMAX) rejection features (c) *Ant3:* UWB with dual band (WiMAX and WLAN) rejection features (d) *Ant4:* UWB with triple band (WiMAX, WLAN, and ITU) rejection features.

respectively. Slots of various shapes are introduced to achieve the band stop characteristics. The inverted-U shaped slot with dimensions of 11 mm x 0.2 mm is applied to reject the ITU frequency band (7.92–8.31 GHz). The inverted-C shaped slot with dimensions of 19.6 mm x 0.3 mm is inserted to suppress the WLAN frequency band (5.18–5.73 GHz). A 13.5 mm x 0.5 mm rectangular slot is introduced for rejecting the WiMAX frequency band (3.01–3.68 GHz).

The frequency of operation of the proposed patch antenna depends on the permittivity of substrate ϵ_r and the length L of the radiating element. The final design is depicted in Figure 1(d). The size of the three geometrical slots is dependent on the stop-band frequency and the dielectric constant of the substrate (ϵ_r). Based on the work in [34] the length of slot1 is quarter wavelength at the stop frequency and can be deduced by (1). According to the research in [35] the lengths of slot2 and slot3 are half wavelength at the stop frequencies and each length is attained by (2).

$$L_{s1} = \frac{c}{4 f_n \sqrt{(\varepsilon_r + 1)/2}} \tag{1}$$

$$L_{s2} = L_{s3} = \frac{c}{2 f_n \sqrt{(\varepsilon_r + 1)/2}} \tag{2}$$

where L_{s1} is the length of a rectangular slot (mm), L_{s2} is the length of inverted-C slot (mm), L_{s3} is the length of inverted-U slot (mm), c is speed of light (3×10^8 m/s) and f_n is the notch frequency (GHz), and ε_r is the dielectric constant of the material (unit less). The design parameters of the antenna are summarized in Table 2.

Table 2: Dimensions of the proposed UWB antenna.

Parameter	Value (mm)	Parameter	Value (mm)	Parameter	Value (mm)
L	32	l_5	9	h_4	5.6
W	30	l_6	13.5	w_1	3
l_1	4.9	l_g	10.2	w_2	4
l_2	1.2	h_1	7.8	w_3	0.5
l_3	3	h_2	13.5	w_f	2.6
l_4	2.3	h_3	3.2	d	26

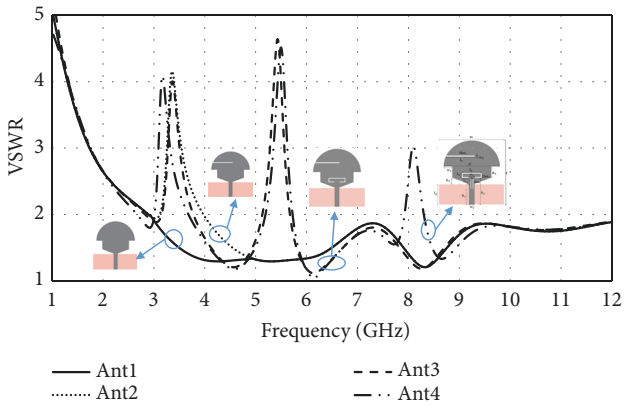

Figure 2: Comparison of simulated VSWR of the proposed UWB antenna.

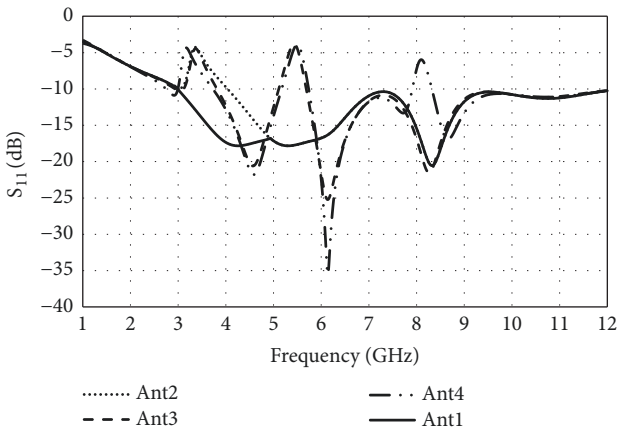

Figure 3: Comparison of simulated S_{11} of the proposed UWB antenna.

The simulated voltage standing wave ratio (VSWR) and reflection coefficient (S_{11}) of the UWB antenna with single notched (Ant1), dual notched (Ant2), and proposed triple notched (Ant3) characteristics are illustrated in Figures 2 and 3, respectively. It is evident from Figure 2 that the Ant1 gives an UWB response (VSWR<2) in the entire 3-10 GHz frequency band. The VSWR> 4 at 3.5 GHz for Ant2 to stop the WiMAX frequency band. For Ant3, the VSWR>4 at 3.5 GHz and 5.4 GHz and hence restricts the WiMAX and WLAN frequency bands. Ant4 gives stop-band characteristics in three frequency bands with a VSWR>4 at 3.5 GHz and 5.4 GHz and VSWR = 3 at 8.2 GHz. The reflection coefficient of Ant1 is less than -10 dB (i.e., S_{11} < -10 dB) in the 3-10 GHz frequency band. The insertion of rectangular slot, inverted-C slot, and inverted-U slot results in band stop characteristics (S_{11} ≥ -5 dB) at 3.5 GHz, 5.4 GHz, and 8.2 GHz, respectively.

3.2. Parametric Study. The parametric study was accomplished by observing the variations in VSWR with the variation in different parts of the antenna such as length of the ground plane (L_g), gap between the ground plane and the radiating patch (h_3), diameter of the circular patch (d), and length of the three slots (i.e., rectangular: $L_{s1} = l_6$, Inverted-C: $L_{s2} = 2l_3 + 2l_4 + l_5$ and Inverted-U: $L_{s3} = 2l_1 + l_2$). The variations in bandwidth and impedance mismatch were observed for various sizes of the ground plane, i.e., l_g = 7.2 mm, 10.2 mm, and 13.2 mm. The VSWR is relatively

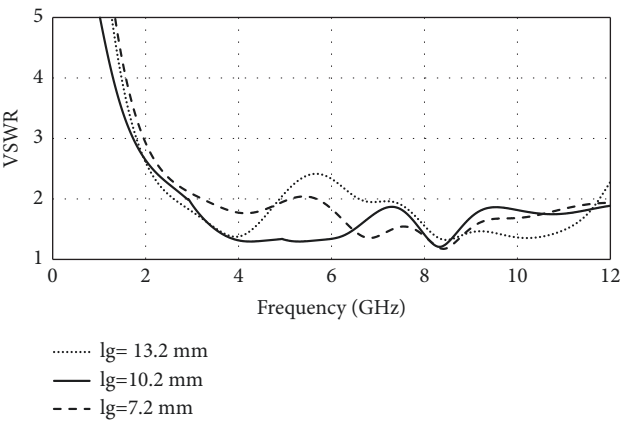

Figure 4: Simulated VSWR by varying the length of the ground plane.

better (<2) in the 3-10 GHz band for l_g = 10.2 mm (Figure 4). The mismatch losses have been increased in the 5-7.5 GHz frequency band for the smaller (7.2 mm) and larger (13.2 mm) values of l_g due to which the VSWR has been degraded. When the diameter (d) of the half circular disc is varied from 22 to 30 mm, variations in the VSWR of the antenna are observed as shown in Figure 5. Relatively better response (VSWR<2 in the 3-10 GHz band) is observed for d = 26 mm. The impedance matching is poor for larger value of d = 30 mm, due to which the VSWR has crossed the threshold of 2 in the 5-7 GHz frequency band. The gap between the

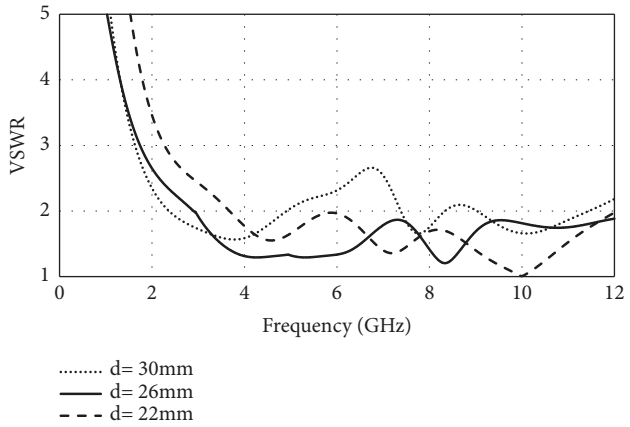

Figure 5: Simulated VSWR by varying the diameter of the radiating patch.

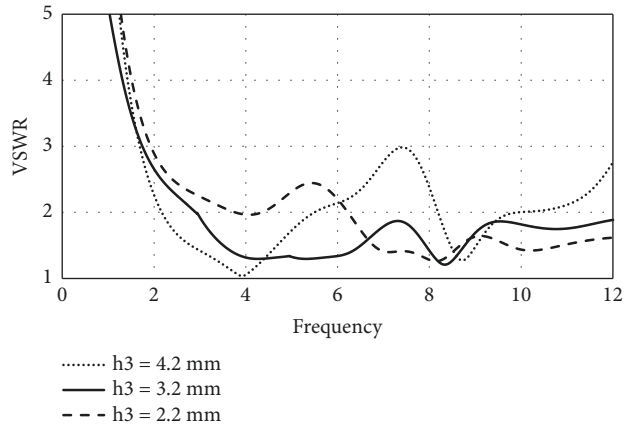

Figure 6: Simulated VSWR for different values of gap between ground and radiating patch.

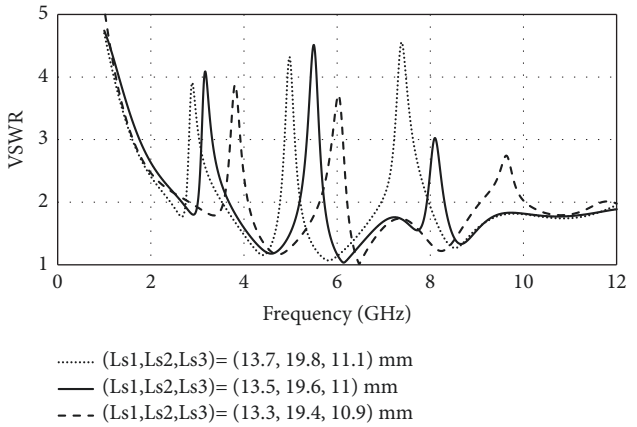

Figure 7: Simulated VSWR for various slot lengths ($L_{s1} = l_6$, $L_{s2} = 2l_3 + 2l_4 + l_5$, $L_{s3} = 2l_1 + l_2$).

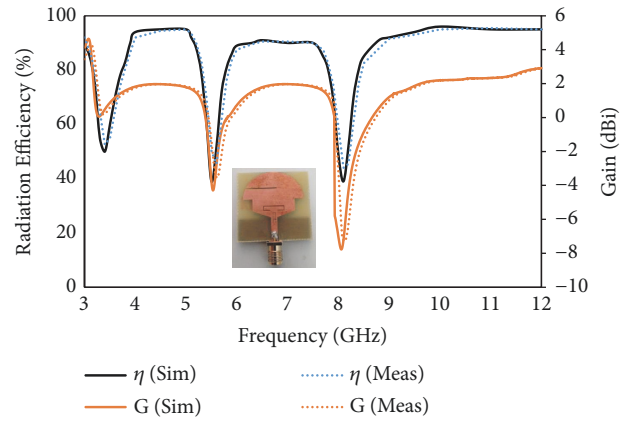

Figure 8: Comparison of simulated and measured radiation efficiency (η) and gain (G) of the proposed tri band-notched UWB antenna.

ground and radiator (h_3) is an important parameter to be optimized. Satisfactory VSWR (<2) has been obtained for h_3 = 3.2 mm (Figure 6). The VSWR is drastically affected if this gap is increased or decreased by 1 mm. This gap controls the mutual coupling between the radiating element and the truncated ground plane, which indirectly configure the input impedance of the antenna. The input impedance of the antenna deviates from the feedline impedance for 2.2 mm and 4.2 mm due to which the standing wave ratio exceeds 2 in the 5-6 GHz and 7-8 GHz frequency bands, respectively. The most critical parameter for optimizing the stop-band of the proposed antenna is the relative lengths of the three slots, previously defined. The desired band-notched characteristics (VSWR>3) are obtained at WiMAX (3.5 GHz), WLAN (5.4 GHz), and ITU (8.2 GHz) frequency bands if the slot lengths are set to (L_{s1}, L_{s2}, and L_{s3}) = (13.5 mm, 19. 6 mm, and 11 mm) as shown in Figure 7; when the lengths of the slots are decreased relative to the above mentioned, the three stop bands are shifted to higher frequencies. Contrary to this, if the lengths of the slots are increased, the stop bands are shifted to lower frequencies.

4. Results

The design is capable of operating in UWB frequency range which is justified from the Figure 2. The antenna is resonating from 2.80 GHz to 12 GHz with VSWR < 2. The objective of this work was to achieve a VSWR of less than 2 for UWB frequency range except the stop bands. The stop bands are WiMAX ranging from 3.01 − 3.68 GHz, the band of WLAN ranging from 5.18 − 5.73 GHz, and ITU8 frequency band ranging from 7.7 − 8.5 GHz which is illustrated in Figures 2 and 3. The simulated and measured gain and radiation efficiency are compared in Figure 8. It can be noted that the gain at the stop-band frequencies is less than that at other frequencies in the UWB spectrum; i.e., the gain obtained at stopbands of 3.5 GHz, 5.4 GHz, and 8.2 GHz is 0 dBi, −4 dBi, and −7.8 dBi, respectively. The radiation efficiency is poor at stop-band frequencies (i.e., 48% at 3.5 GHz, 40% at 5.4 GHz, and 42% at 8.2 GHz). The antenna radiates efficiently (>90%) in the rest of the UWB frequency spectrum.

For understanding the stop-band mechanism, the snapshots of vector current distribution and surface current density are shown in Figures 9 and 10, respectively. It is evident

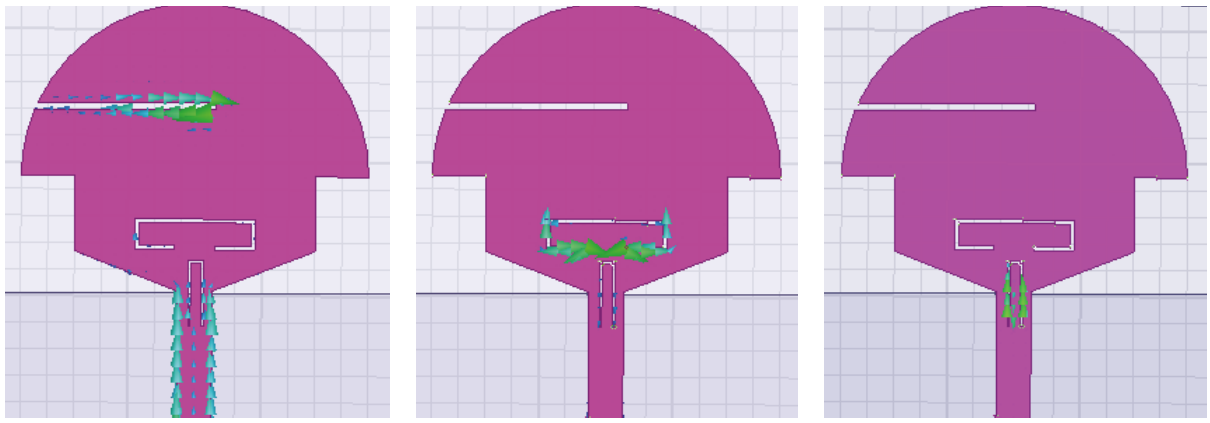

(a) (b) (c)

Figure 9: Vector current distribution of the UWB antenna (a) 3.5 GHz, (b) 5.4, and (c) 8.2 GHz.

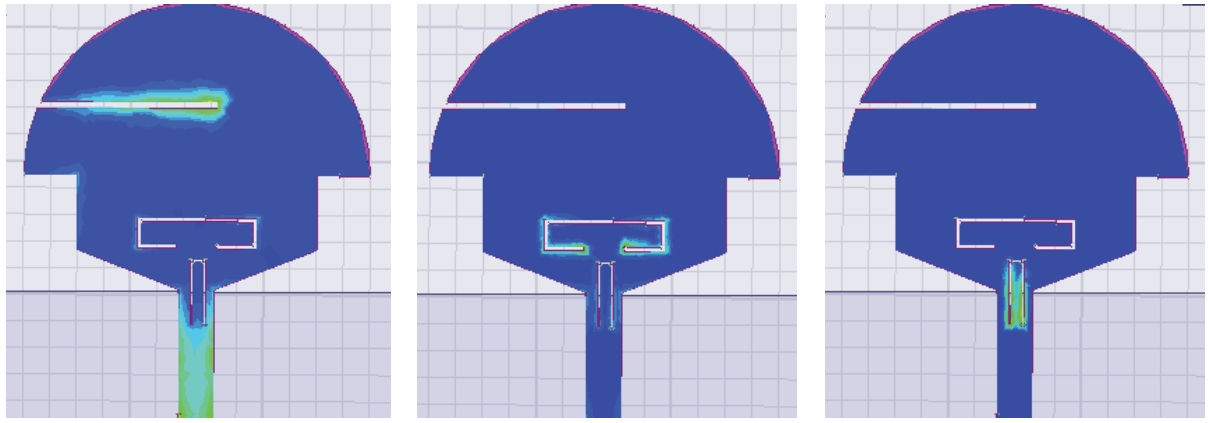

(a) (b) (c)

Figure 10: Surface current density of the UWB antenna (a) 3.5 GHz, (b) 5.4 GHz, and (c) 8.2 GHz.

from these plots that the surface currents flow in opposite direction along the sides of the rectangular, inverted-C, and inverted-U shaped slots, at stop-band frequencies of 3.5 GHz, 5.4 GHz, and 8.2 GHz. The combined effect is cancellation of the resultant surface current due which the antenna not only radiate less efficiently (<50%) but also gives very poor gain (<0 dB) at these frequencies. The surface currents at radiating frequencies such as 4 GHz, 7 GHz, and 9 GHz are denser on other parts of the radiating patch and are depicted in Figure 11.

The proposed antenna is fabricated in order to validate the simulations. The front and back view of the fabricated design is depicted in Figure 12. The comparison of simulated and measured S_{11} is depicted in Figure 13 while the comparison of measured and simulated VSWR values is given in Figure 14. The antenna gives better driving-point impedance bandwidth (S_{11} <-10 dB and VSWR<2) in the whole UWB spectrum except the three stop-band frequencies. From the measured results, a small shift in notched frequencies is noted, the antenna resonates from 2.78 to 10.7 *GHz*, the stop-band for ITU applications (7.92 – 8.31 *GHz*) is shifted to 7.7 – 8.5 *GHz*, the stop-band reserved for WLAN (5.18 – 5.73 *GHz*) is shifted to 5 – 5.8 *GHz*, and the stop-band of 3.01 – 3.68 *GHz* is moved to 3.1 – 4.02 *GHz*. The simulated and measured radiation pattern of the antenna at 4, 7, and 9 GHz frequencies in both principal planes {E-plane (*YZ* @ϕ = 90°) and H-plane (*XZ* @ϕ = 0°)} has been compared in Figure 15. At 4 GHz the radiation pattern forms a "figure of eight" in the YZ-plane with a null occurring at 90°. The pattern is omnidirectional in the XZ-plane at this frequency. The pattern is predominantly omnidirectional in the XZ-plane at 7 GHz, whereas null radiations occur at 90° and 330° in the YZ-plane in this frequency band. The pattern is nearly omni in both principal planes at 9 GHz, with minimum radiation intensity at 0° and 180°.

5. Conclusion and Future Work

In this article, a triple stop-band antenna for UWB applications is designed. The design parameters are optimized to achieve good VSWR response over UWB frequencies. Slots of different shapes have been introduced within the

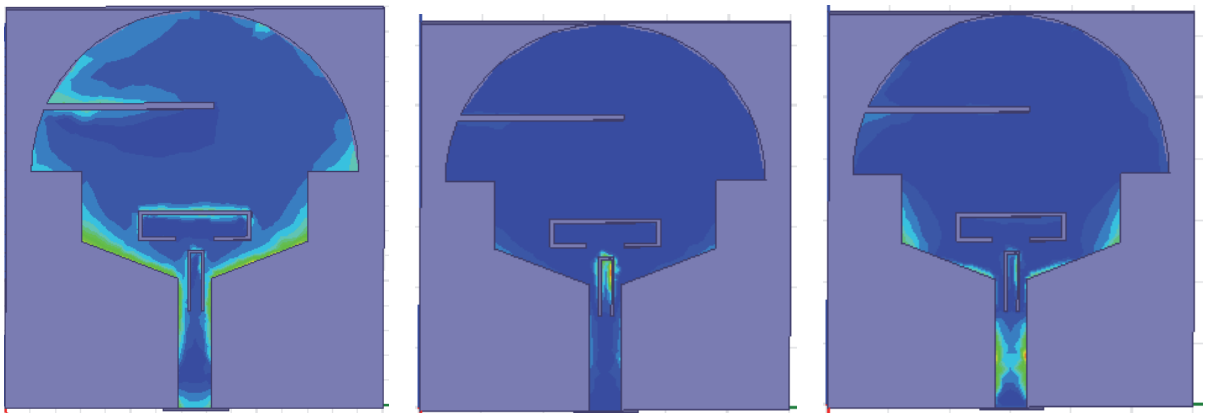

(a) (b) (c)

Figure 11: Surface current of the UWB antenna (a) 4 GHz, (b) 7 GHz, and (c) 9 GHz.

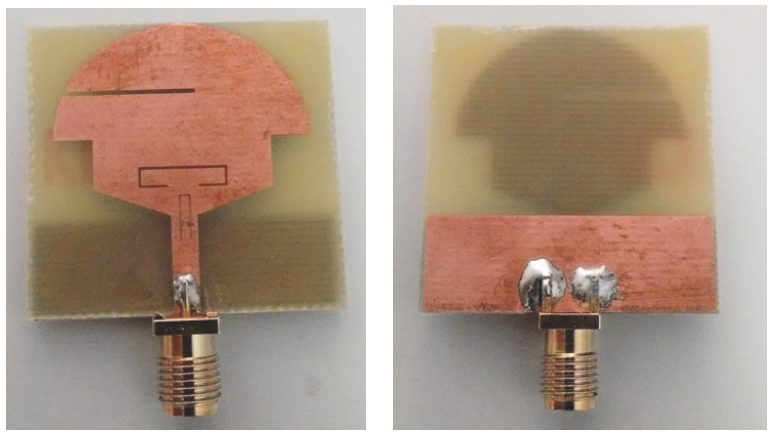

(a) (b)

Figure 12: Photographic image of the fabricated of the UWB antenna. (a) Top view and (b) back view.

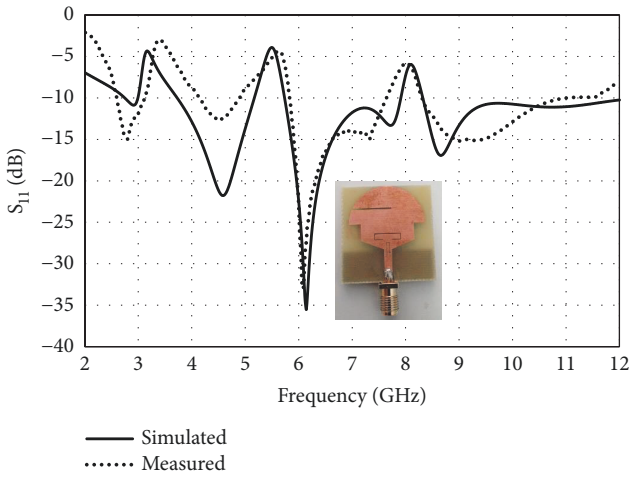

Figure 13: Measured and simulated S_{11} (dB) of the proposed UWB antenna.

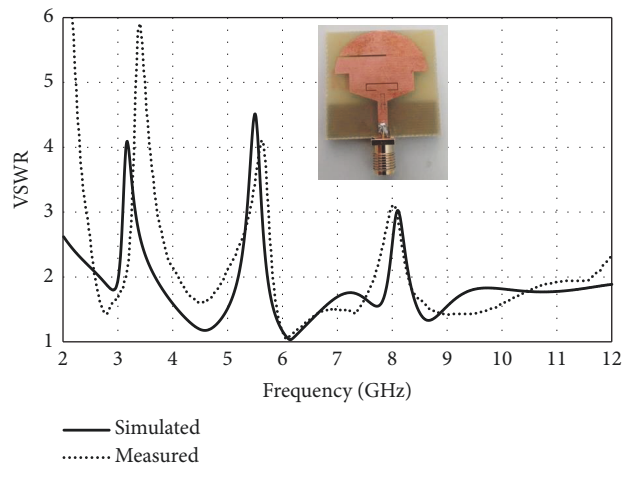

Figure 14: Measured and simulated VSWR of the proposed UWB antenna.

radiating element of the antenna to achieve triple stop bands. The inverted-U, C and rectangular moulded slots are the main contributors to give the stop frequency bands of 7.7—8.5 GHz (ITU band), 5.18—5.73 GHz (WLAN band), and 3.01—3.68 GHz (WiMAX band), respectively. The proposed antenna gives satisfactory gain (>1.95 dBi) and efficiency (>90%) within the unnotched portion of the UWB spectrum. Within the notched frequency bands, the gain

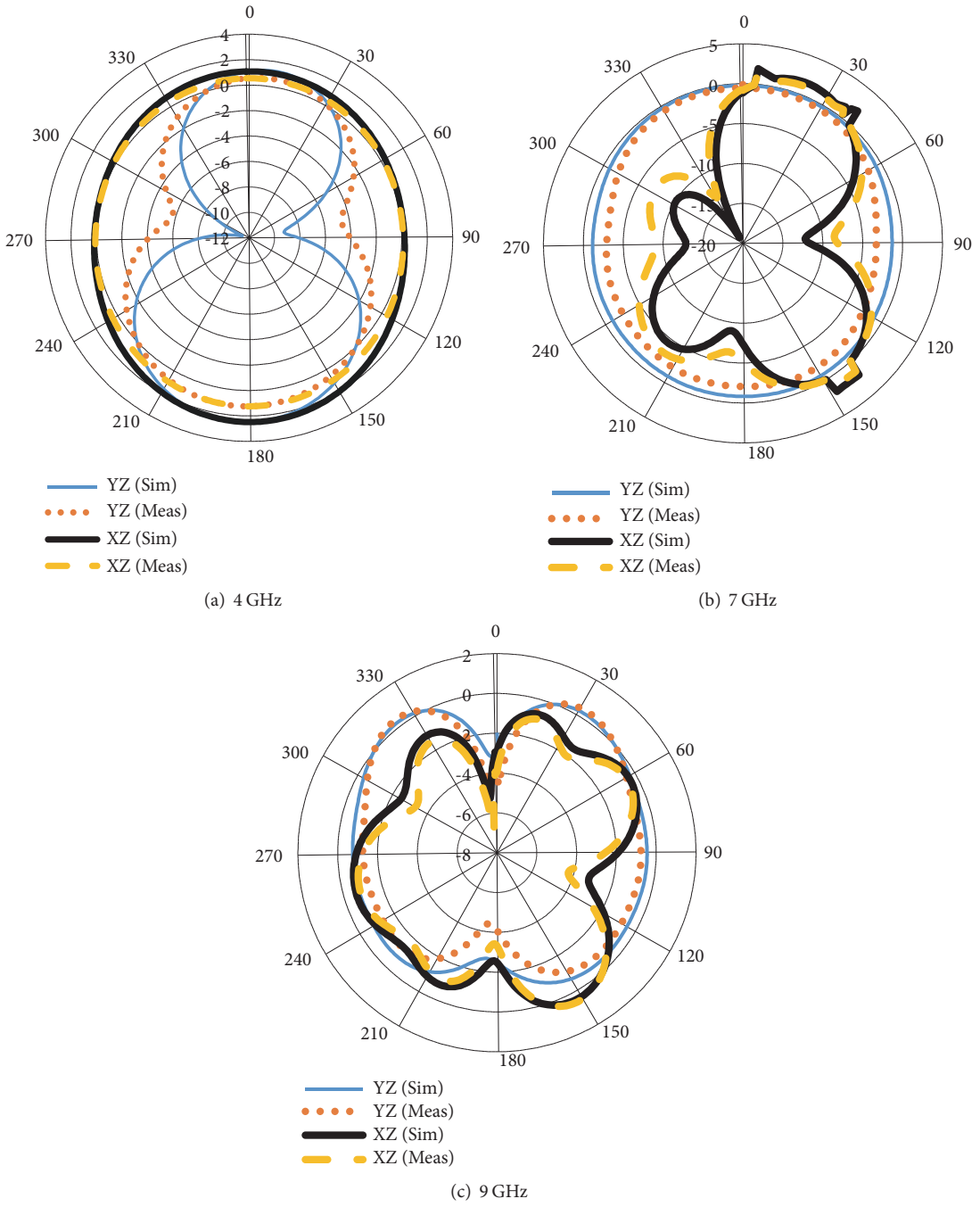

Figure 15: Comparison of simulated and measured radiation pattern in both principal planes at (a) 4 GHz, (b) 7 GHz, and (c) 9 GHz.

and efficiency of the antenna have been significantly reduced below 0 dBi and 50%, respectively. The proposed antenna is fabricated and the simulated results are found in close agreement with the measurements. The proposed antenna is compact and low-profile and can be used in various short-range wireless applications. The gain of the proposed antenna can be increased by making use of novel metasurfaces which can be integrated with the proposed design as a superstrate or reflector. Enhanced gain in particular direction can be realized by using the underlying theory and concept of beam-scanning phase array antennas in the UWB spectrum.

Data Availability

No data were used to support this study.

Conflicts of Interest

The authors declare that there are no conflicts of interest regarding the publication of this paper.

Acknowledgments

This work was supported by the Basic Science Research Program through the National Research Foundation of Korea

(NRF) funded by the Ministry of Education (grant number: NRF-2017R1D1A1B03028350).

References

[1] G. Z. Rafi and L. Shafai, "Wideband V-slotted diamond-shaped microstrip patch antenna," *Electronics Letters*, vol. 40, no. 19, pp. 1166-1167, 2004.

[2] H. G. Schantz, "Ultra wideband technology gains a boost from new antennas," *Antenna Systems & Technology*, vol. 4, no. 1, pp. 25–27, 2001.

[3] A. Acampora and M. Krull, "A new approach to peer-to-peer wireless LANs based on ultra wide band technology," *Wireless Networks*, vol. 14, no. 3, pp. 335–346, 2008.

[4] K. G. Thomas and M. Sreenivasan, "A simple ultrawideband planar rectangular printed antenna with band dispensation," *IEEE Transactions on Antennas and Propagation*, vol. 58, no. 1, pp. 27–34, 2010.

[5] A. M. Abbosh and M. E. Bialkowski, "Design of ultrawideband planar monopole antennas of circular and elliptical shape," *IEEE Transactions on Antennas and Propagation*, vol. 56, no. 1, pp. 17–23, 2008.

[6] R. K. Saraswat and M. Kumar, "A frequency band reconfigurable UWB antenna for high gain applications," *Progress In Electromagnetics Research B*, vol. 64, pp. 29–45, 2015.

[7] Federal Communications Commission, *First report and order, Revision of Part 15 of commission's rule regarding UWB transmission system FCC 02-48*, Washington, DC, USA, April 2002.

[8] S. Roy, J. R. Foerster, V. S. Somayazulu, and D. G. Leeper, "Ultrawideband radio design: the promise of high-speed, short-range wireless connectivity," *Proceedings of the IEEE*, vol. 92, no. 2, pp. 295–311, 2004.

[9] S. Licul, J. A. Noronha, W. A. Davis et al., "A parametric study of time-domain characteristics of possible UWB antenna architectures," in *Proceedings of the IEEE 58th Vehicular Technology Conference*, pp. 3110–3114, October 2003.

[10] J. Kazim, A. Bibi, M. Rauf, and M. Tariq, "A compact planar dual band-notched monopole antenna for UWB application," *Microwave and Optical Technology Letters*, vol. 56, no. 5, pp. 1095–1097, 2014.

[11] M. M. Sharma, J. K. Deegwal, A. Kumar, and M. C. Govil, "Compact planar monopole UWB antenna with quadruple band-notched characteristics," *Progress In Electromagnetics Research*, vol. 47, pp. 29–36, 2014.

[12] N. Jaglan, S. D. Gupta, B. K. Kanaujia, and S. Srivastava, "Band notched UWB circular monopole antenna with inductance enhanced modified mushroom EBG structures," *Wireless Networks*, vol. 24, no. 2, pp. 383–393, 2018.

[13] X. F. Zhu and D. L. Su, "Symmetric E-shaped slot for UWB antenna with band-notched characteristic," *Microwave and Optical Technology Letters*, vol. 52, no. 7, pp. 1594–1597, 2010.

[14] A. A. L. Neyestanak and A. A. Kalteh, "Band-notched elliptical slot uwb microstrip antenna with elliptical stub filled by the h-shaped slot," *Journal of Electromagnetic Waves and Applications*, vol. 22, no. 14-15, pp. 1993–2002, 2008.

[15] A. A. Kalteh, R. Fallahi, and M. G. Roozbahani, "Design of a band-notched microstrip circular slot antenna for UWB communication," *Progress In Electromagnetics Research*, vol. 12, pp. 113–123, 2010.

[16] P. Gao, S. He, X. Wei, Z. Xu, N. Wang, and Y. Zheng, "Compact printed UWB diversity slot antenna with 5.5-GHz band-notched characteristics," *IEEE Antennas and Wireless Propagation Letters*, vol. 13, pp. 376–379, 2014.

[17] S. M. Khan, A. Iftikhar, S. M. Asif, A. D. Capobianco, and B. D. Braaten, "A compact four elements UWB MIMO antenna with on-demand WLAN rejection," *Microwave and Optical Technology Letters*, vol. 58, no. 2, pp. 270–276, 2016.

[18] G. Gao, L. He, B. Hu, and X. Cong, "Novel dual band-notched UWB antenna with T-shaped slot and CSRR structure," *Microwave and Optical Technology Letters*, vol. 57, no. 7, pp. 1584–1590, 2015.

[19] K. G. Jangid, P. K. Jain, B. R. Sharma et al., "CPW fed UWB antenna with enhanced bandwidth and dual band notch characteristics," *AIP Conference Proceedings*, vol. 1953, article 140127, 2018.

[20] M. Nejatijahromi, M. Rahman, and M. Naghshvarianjahromi, "Continuously tunable WiMAX band-notched UWB antenna with fixed WLAN notched band," *Progress In Electromagnetics Research*, vol. 75, pp. 97–103, 2018.

[21] A. Sohail, K. S. Alimgeer, A. Iftikhar et al., "Dual notch band UWB antenna with improved notch characteristics," *Microwave and Optical Technology Letters*, vol. 60, no. 4, pp. 925–930, 2018.

[22] B. Li and J. S. Hong, "Design of two novel dual band-notched UWB antennas," *International Journal of Antennas and Propagation*, vol. 2012, Article ID 303264, 7 pages, 2012.

[23] R. Shi, X. Xu, J. Dong, and Q. Luo, "Design and analysis of a novel dual band-notched UWB antenna," *International Journal of Antennas and Propagation*, vol. 2014, Article ID 531959, 10 pages, 2014.

[24] P. S. Bakariya, S. Dwari, and M. Sarkar, "A triple band notch compact UWB printed monopole antenna," *Wireless Personal Communications*, vol. 82, no. 2, pp. 1095–1106, 2015.

[25] D. Yadav, M. P. Abegaonkar, S. K. Koul, V. Tiwari, and D. Bhatnagar, "A compact dual band-notched UWB circular monopole antenna with parasitic resonators," *AEU-International Journal of Electronics and Communications*, vol. 84, pp. 313–320, 2018.

[26] M. Almalkawi and V. Devabhaktuni, "Ultrawideband antenna with triple band-notched characteristics using closed-loop ring resonators," *IEEE Antennas and Wireless Propagation Letters*, vol. 10, pp. 959–962, 2011.

[27] F. Zhu, S. Gao, A. T. S. Ho et al., "Multiple band-notched UWB antenna with band-rejected elements integrated in the feed line," *IEEE Transactions on Antennas and Propagation*, vol. 61, no. 8, pp. 3952–3960, 2013.

[28] S. Kundu and S. K. Jana, "Leaf-shaped CPW-fed UWB antenna with triple notch bands for ground penetrating radar applications," *Microwave and Optical Technology Letters*, vol. 60, no. 4, pp. 930–936, 2018.

[29] J. Banerjee, A. Karmakar, R. Ghatak, and D. R. Poddar, "Compact CPW-fed UWB MIMO antenna with a novel modified Minkowski fractal defected ground structure (DGS) for high isolation and triple band-notch characteristic," *Journal of Electromagnetic Waves and Applications*, vol. 31, no. 15, pp. 1550–1565, 2017.

[30] N. Jaglan, S. D. Gupta, E. Thakur, D. Kumar, B. K. Kanaujia, and S. Srivastava, "Triple band notched mushroom and uniplanar EBG structures based UWB MIMO/Diversity antenna with enhanced wide band isolation," *AEÜ - International Journal of Electronics and Communications*, vol. 90, pp. 36–44, 2018.

[31] M. Yoo and S. Lim, "SRR-and CSRR-loaded ultra-wideband (UWB) antenna with tri-band notch capability," *Journal of Electromagnetic Waves and Applications*, vol. 27, no. 17, pp. 2190–2197, 2013.

[32] S.-Y. Suh, W. L. Stutzman, W. A. Davis et al., "A UWB antenna with a stop-band notch in the 5-GHz WLAN band," in *Proceedings of the IEEE/ACES International Conference on Wireless Communications and Applied Computational Electromagnetics*, pp. 203–207, IEEE, 2005.

[33] A. Darvazehban, O. Manoochehri, M. A. Salari, P. Dehkhoda, and A. Tavakoli, "Ultra-wideband scanning antenna array with Rotman lens," *IEEE Transactions on Microwave Theory and Techniques*, vol. 65, no. 9, pp. 3435–3442, 2017.

[34] Z. A. Zheng and Q. X. Chu, "Compact CPW-fed UWB antenna with dual band-notched characteristics," *Progress In Electromagnetics Research*, vol. 11, pp. 83–91, 2009.

[35] Q. X. Chu and Y. Y. Yang, "A compact ultrawideband antenna with 3.4/5.5 GHz dual band-notched characteristics," *IEEE Transactions on Antennas and Propagation*, vol. 56, no. 12, pp. 3637–3644, 2008.